Explicit Precipitation-Type Diagnosis from a Model Using a Mixed-Phase Bulk Cloud–Precipitation Microphysics Parameterization

STANLEY G. BENJAMIN, JOHN M. BROWN, AND TATIANA G. SMIRNOVA*

NOAA/Earth System Research Laboratory, Boulder, Colorado

(Manuscript received 8 October 2015, in final form 20 January 2016)

ABSTRACT

The Rapid Refresh (RAP) and High-Resolution Rapid Refresh (HRRR), both operational at NOAA's National Centers for Environmental Prediction (NCEP) use the Thompson et al. mixed-phase bulk cloud microphysics scheme. This scheme permits predicted surface precipitation to simultaneously consist of rain, snow, and graupel at the same location under certain conditions. Here, the explicit precipitation-type diagnostic method is described as used in conjunction with the Thompson et al. scheme in the RAP and HRRR models. The postprocessing logic combines the explicitly predicted multispecies hydrometeor data and other information from the model forecasts to produce fields of surface precipitation type that distinguish between rain and freezing rain, and to also portray areas of mixed precipitation. This explicit precipitation-type diagnostic method is used with the NOAA operational RAP and HRRR models. Verification from two winter seasons from 2013 to 2015 is provided against METAR surface observations. An example of this product from a January 2015 south-central United States winter storm is also shown.

1. Introduction

Diagnosis of precipitation type from weather forecast model predictions is important for public forecasting of winter storms, and also for air and surface transportation, energy, hydrology, and other applications. The advent of mixed-phase bulk microphysics schemes in some NOAA operational numerical prediction models [Rapid Update Cycle (RUC; Benjamin et al. 2004a,b); Rapid Refresh (RAP; Benjamin et al. 2016); and High-Resolution Rapid Refresh (HRRR; Smith et al. 2008; Benjamin et al. 2016)] enabled a relatively direct diagnosis of precipitation type [e.g., rain *R*, snow *S*, ice pellets (IP), freezing rain and drizzle (FZ), and mixed types] at the surface. Since 1998, the RUC model running at NOAA's National Centers for Environmental Prediction (NCEP) has used a bulk scheme in which separate mixing ratios for cloud water, rainwater, ice, snow, and graupel are predicted at each 3D grid point. From 2005 to 2012, the scheme used in RUC was as described by Thompson et al. (2004). The RAP, which replaced the RUC at NCEP on 1 May 2012, uses a more advanced version (Thompson et al. 2008). RAP, version 3, and HRRR, version 2, planned for implementation at NCEP in 2016 and running at Earth System Research Laboratory (ESRL) starting in April 2015 (Benjamin et al. 2016, their Table 1), use an aerosol-aware version of the Thompson et al. scheme (Thompson and Eidhammer 2014). This use of multispecies mixed-phase microphysics in the RUC, RAP, and HRRR models was motivated by a need to improve the forecast skill for clouds, in general, and supercooled liquid water, in particular, for aviation requirements. Here, we describe the diagnostic precipitation-type scheme used in the NCEP RAP, version 3, and HRRR, version 2. This precipitation-type scheme is a recent alternative to profile-based diagnostic methods summarized in section 2. Ikeda et al. (2013) presented verification results on precipitation-type forecasts from an earlier version of HRRR as of 2012. This paper is an expansion on and correction of their Table 1 and includes an examination of more recent explicit precipitation-type results.

The RAP and HRRR models use the community NCEP Unified Post Processor (UPP) also used for other models. Options have been added to UPP including

* Additional affiliation: Cooperative Institute for Research in Environmental Sciences, University of Colorado, Boulder, Colorado.

Corresponding author address: Stanley G. Benjamin, NOAA/ESRL, R/GSD1, 325 Broadway, Boulder, CO 80305-3328.
E-mail: stan.benjamin@noaa.gov

DOI: 10.1175/WAF-D-15-0136.1

ceiling (cloud-base height), visibility, and precipitation type, designed for microphysics schemes with multiple prognostic hydrometeor-species variables. In this paper, we describe the UPP option for this explicit, multispecies diagnostic of precipitation type, which is currently applied only in the RAP and HRRR.

2. Other precipitation-type diagnostic schemes

Well before the introduction of mixed-phase microphysics schemes into some operational numerical weather prediction models, successful diagnostic techniques were designed using implicit assumptions about microphysical processes to allow estimation of the precipitation type. These procedures can be grouped into 1) algorithmic or decision-tree approaches based on an observed or predicted sounding and 2) statistical procedures that make use of a training dataset to derive a set of equations that is then applied to predicted fields. All of the diagnostic schemes discussed here are for discrete yes/no identification of each precipitation type, the same yes or no designation in observer guidelines in the NOAA Federal Meteorological Handbook No. 1 (OFCM 2005, chapter 8).

a. *Algorithmic approaches*

A number of simple but effective algorithms have been developed that use as input model-forecast profiles of temperature and relative humidity from the surface upward to the level of assumed precipitation-generating layers aloft. The algorithms used most often by forecasters in North America are those developed by Ramer (1993) and Baldwin et al. (1994). A description of Ramer's algorithm can be found in Bourgouin (2000), Wandishin et al. (2005), and DeGaetano et al. (2008). (The latter paper introduces some modifications to Ramer's algorithm for application to forecasts of ice accretion.) In essence, Ramer's approach is to define an ice fraction of the precipitation in a precipitation-generation layer and, based on the temperature of that layer, assume the ice fraction of this precipitation is either 0 (liquid) or 1 (frozen). Then, for the frozen case, a decision tree that depends on the wet-bulb temperature profile is used to modify the ice fraction as a function of height between the base of the generating layer and the ground. The value of the ice fraction then determines the precipitation type.

The Baldwin et al. algorithm also considers the vertical profile of the wet-bulb temperature below saturated layers where precipitation is presumed to form. If this precipitation is presumed frozen, the precipitation type at the surface is obtained by using the vertically integrated departure of the wet-bulb temperature from 0°C in various layers and the temperature in the lowest model layer. A more complete description can be found in Bourgouin (2000) and Wandishin et al. (2005).

b. *Statistical approaches*

Among statistical approaches of which we are aware, the earliest to use upper-air data is that of Wagner (1957). Using surface aviation observations of precipitation type and collocated rawinsonde observations (about 40 stations), Wagner compared the thickness of the 1000–500-hPa layer to the occurrence of frozen precipitation and determined the thickness values corresponding to a 50% probability of frozen precipitation. The thickness values so obtained are still used by many forecasters as a point of comparison with predicted thickness values.

The model output statistics (MOS) approach for precipitation type was first applied by Bocchieri (1979, 1980) and Bocchieri and Maglaras (1983) to the then-operational Limited Area Fine Mesh (LFM) model. Since then, there have been many upgrades, and MOS is now applied to output from the Global Forecast System (GFS) as well as the North American Mesoscale Forecast System (NAM) models for precipitation-type purposes. Perfect-prog (Vislocky and Young 1989) approaches include Keeter and Cline (1991) and Bourgouin (2000). Keeter and Cline used radiosonde 1000–700-, 1000–850-, and 850–700-hPa thickness values at Raleigh–Durham, North Carolina, regressed against collocated surface observations. The approach of Bourgouin (2000) classified sounding temperature profiles into four groupings (freezing rain or ice pellets, ice pellets or rain, snow or rain, and snow) and derived statistics separately for each grouping. Separate positive and negative areas on a thermodynamic diagram between the 0°C isotherm and the observed temperature profile are computed for each sounding in the training dataset and are determined to be important predictors. Bourgouin considers his approach most applicable to synoptic situations characterized by broad synoptic-scale lift leading to widespread, deep saturation. Manikin (2005) combined the Baldwin et al., Ramer, Bourgouin, and revised Baldwin et al. algorithms into a single predominant precipitation-type value now used often in NCEP models (http://www.wpc.ncep.noaa.gov/wwd/impactgraphics/).

A recent contribution by Schuur et al. (2012) shares conceptual aspects with the earlier algorithmic approaches as well as that of Bourgouin in that it classifies vertical profiles (modeled or observed) according to the number of 0°C crossings by the wet-bulb vertical temperature profile together with the 2-m temperature. This method considers local extrema of this profile between the intermediate 0°C crossings. This algorithmic

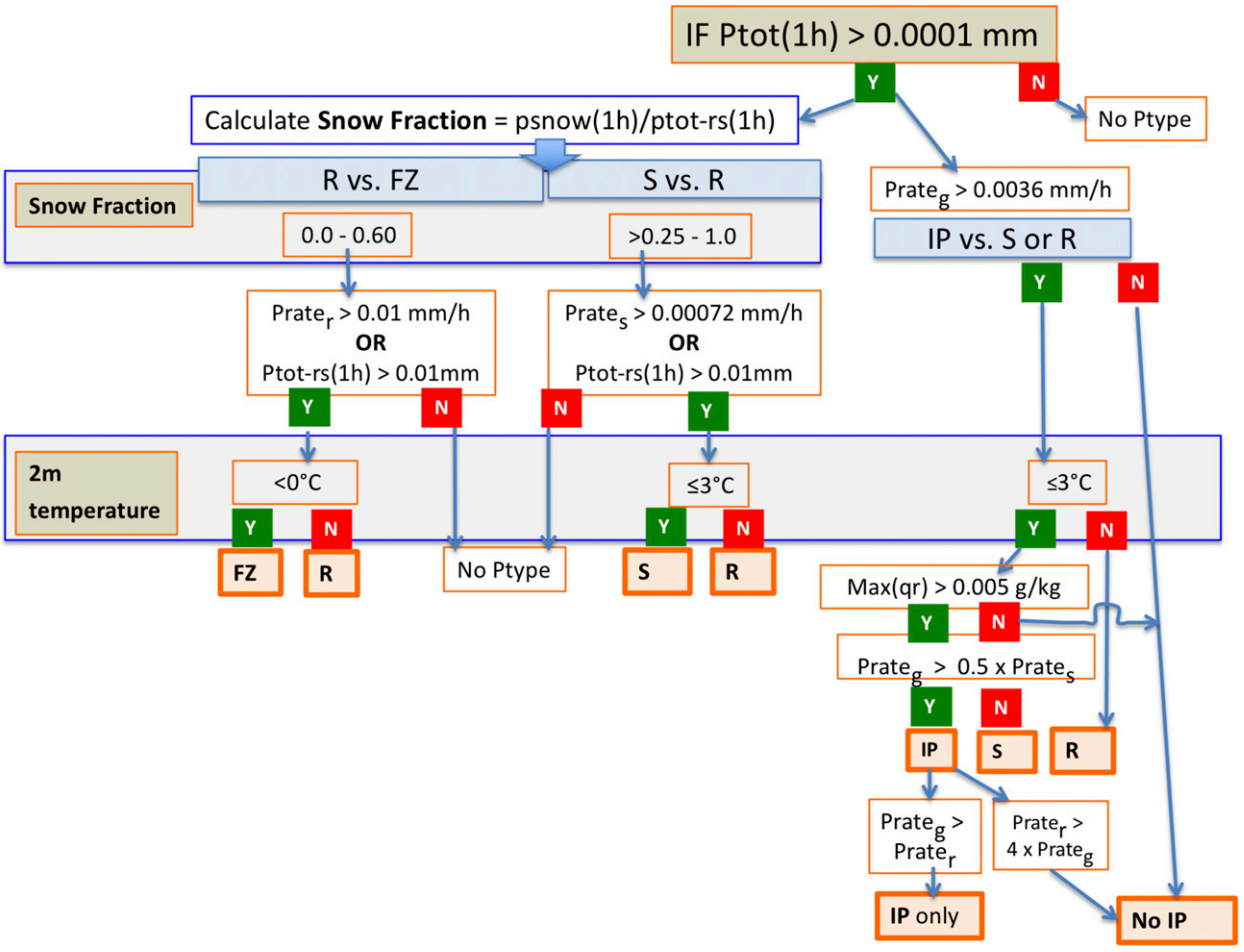

FIG. 1. Flowchart describing the diagnostic logic for determination of precipitation type where Ptot, Ptot-rs, and Psnow are the total, rain plus snow only (no graupel), and snow only (water equivalent) precipitation, respectively, with 1 h indicating over the last hour. The instantaneous fall rate for different hydrometeor types is given by Prate where the subscript indicates the type of hydrometeor. The max rain mixing ratio in the column is represented by Max(qr).

approach could stand alone but is intended for use in conjunction with polarimetric radar, in which the radar polarimetric parameters indicate whether a bright band (i.e., a melting layer) exists. If such a layer is detected, then the precipitation type at the ground is expected to be rain, freezing rain, ice pellets, or a mixture of freezing rain and ice pellets, or possibly even wet (melting) snow if the melting level is detected at the lowest elevation scan, but not dry snow.

3. Explicit diagnostic scheme for precipitation type

In the postprocessing algorithm described here, separate yes/no indicators are diagnosed for each of four different precipitation-type categories: rain, snow, ice pellets (including graupel), and freezing rain. These yes/no indicators are determined from the explicit 3D hydrometeor mixing ratios reaching the ground as calculated in the cloud microphysics parameterization (Thompson et al. 2008; Thompson and Eidhammer 2014) in the RAP or HRRR models [or from the Thompson et al. (2004) scheme in the RUC model]. The hydrometeor fields predicted by the Thompson et al. schemes are mixing ratios of cloud water (droplets), rain, cloud ice, snow, and graupel, as well as the number concentration of raindrops and cloud-ice particles.[1] These hydrometeor mixing ratio prognostic fields undergo horizontal transport as well as vertical transport at appropriate fall speeds. The precipitation-type diagnostic algorithm described here makes use of the explicit precipitation of rain, snow, and graupel predicted to reach the surface by

[1] The number concentration of cloud water drops is also predicted in the Thompson–Eidhammer aerosol-aware scheme but is not used in the precipitation identification described here.

the model. Using continuous model-provided explicit fields of hydrometeor mixing ratios and fall rates (mass accumulation at ground per unit time), this algorithm estimates thresholds for these parameters to approximate the same discrete yes/no observer guidelines in the NOAA Federal Meteorological Handbook No. 1 (OFCM 2005, chapter 8).

The explicit precipitation-type scheme described here depends on the microphysics scheme to provide a "first guess" of precipitation types reaching the ground. (Note that because rain, snow, and graupel are each predicted separately by the forecast model, i.e., each possessing separate mixing ratios and fall speeds, it is possible for the model to predict that two or more of these types will reach a given point on the ground simultaneously.) For each allowable precipitation type in this diagnostic scheme (rain, snow, ice pellets, and freezing rain), the model output within each grid column (not just at the surface) is used to derive a separate yes/no (1/0) decision on whether that type is reaching the ground. These precipitation-type values from the postprocessing are not mutually exclusive, except for rain versus freezing rain. More than one value (as many as three) can be yes (1) at a given grid point at a given time.

a. Diagnostic logic flowchart for precipitation types

The sequence of the diagnostic logic is depicted completely in the flowchart in Fig. 1, with further discussion below. The rationale for this scheme is provided in the following subsection. Each model grid column is considered separately, and all precipitation rates below are at the ground and in liquid-water equivalent. After determining if there was even a minimal amount of precipitation during the last hour (including that from parameterized convection, if appropriate, using 0°C as a snow/rain threshold), the explicit precipitation-type diagnosis logic is treated for three decisions: rain versus freezing rain/drizzle, snow versus rain, and ice pellets versus rain or snow. Each treatment allows consideration of instantaneous precipitation (via fall rates for rain, snow, or graupel) and precipitation over the last hour.

Some of the precipitation-type rules are based on a snow fraction (SF) defined as the mass of snow accumulation divided by the combined mass of snow and rain. The snow fraction is calculated at each grid point for accumulation over some previous forecast period. These precipitation accumulations are updated each time step from the near-surface mixing ratio times the fall speed, as described in Thompson et al. (2008) and Thompson and Eidhammer (2014). In the RAP and HRRR, the previous forecast period is currently 1 h but can be set to shorter time periods (e.g., 15 min).

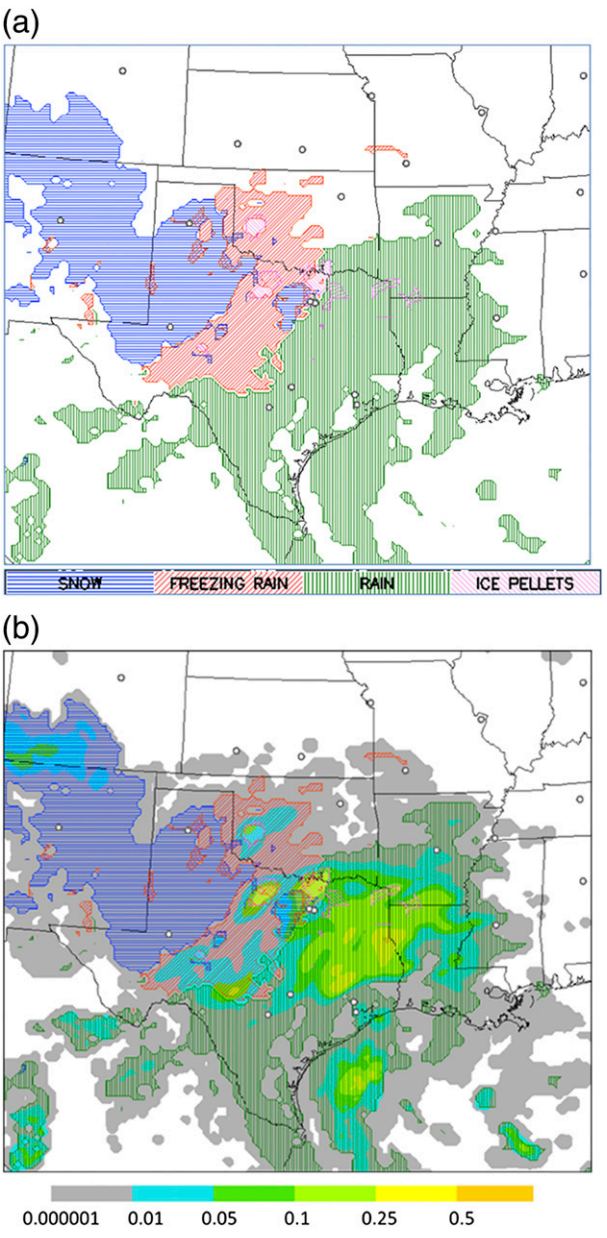

FIG. 2. Precipitation type [snow (blue horizontal hatched lines), rain (green vertical hatched lines), freezing rain (red sloping upward to right hatched lines), and ice pellets (lavender sloping downward to right hatched lines)] from a 1-h forecast from an experimental version of the RAP using the explicit diagnostic method. The RAP 1-h forecast is valid at 1600 UTC 1 Jan 2015 and was initialized at 1500 UTC, 1 h earlier. Note that precipitation type is indicated for areas with 1-h precipitation (water equivalent) less than 0.01 in. (0.25 mm) because precipitation type can be diagnosed with 1-h precipitation as low as 0.0001 mm. Circles shown are for major airports. (a) Results are given without total 1-h precipitation. (b) Results are given with total 1-h precipitation (in.; water equivalent).

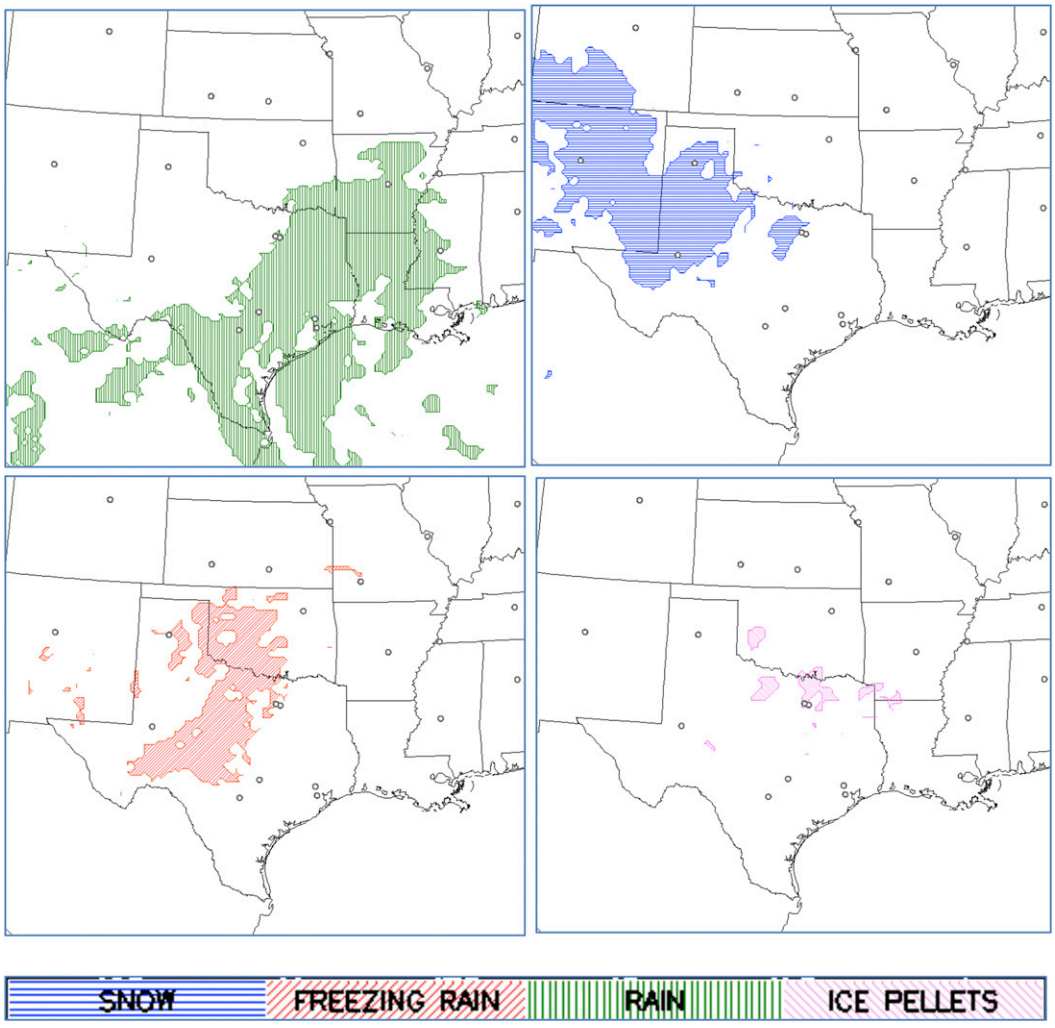

FIG. 3. As in Fig. 2, but for precipitation-type forecasts shown separately for each precipitation type with (top left) rain, (top right) snow, (bottom left) freezing rain, and (bottom right) ice pellets.

1) SNOW VERSUS RAIN

If SF > 0.25 and either the current snow precipitation rate is $>0.000\,72\,\text{mm}\,\text{h}^{-1}$ ($0.2 \times 10^{-9}\,\text{m}\,\text{s}^{-1}$) (liquid equivalent) or the total precipitation of rain plus snow during the previous hour is >0.01 mm, snow is diagnosed as long as the current 2-m temperature (from the model forecast) is <3°C. If the 2-m temperature is ≥ 3°C, rain is diagnosed instead.

2) RAIN VERSUS FREEZING RAIN

If SF < 0.6 and either the current rain rate at the ground is at least $0.01\,\text{mm}\,\text{h}^{-1}$ or there has been at least 0.01-mm total precipitation of rain plus snow during the previous hour, then rain or freezing rain is diagnosed. If the 2-m temperature is <0°C, freezing rain/drizzle is diagnosed; otherwise, rain is diagnosed.

3) ICE PELLETS AND RELATED DEPENDENCIES

Dependencies regarding IP diagnosis are more complicated as a result of the attempt to match observing guidelines as described earlier in section 3. If the current fall rate for graupel is $>0.0036\,\text{mm}\,\text{h}^{-1}$ ($1.0 \times 10^{-9}\,\text{m}\,\text{s}^{-1}$), ice pellet precipitation is generally diagnosed, but with further dependencies including 2-m temperature and relative instantaneous fall rates for graupel, rain, and snow. First, for IP, the graupel fall rate at the surface must be greater than that for snow; otherwise, S is diagnosed and not IP. Also to limit IP diagnosis to situations with conditions normally expected, there must be a level aloft with the rain mixing ratio $>0.005\,\text{g}\,\text{kg}^{-1}$. [Note that with a previous maximum rain mixing ratio set as $>0.05\,\text{g}\,\text{kg}^{-1}$, IP was rarely diagnosed (Elmore et al. 2015), resulting in this modification.] If, in

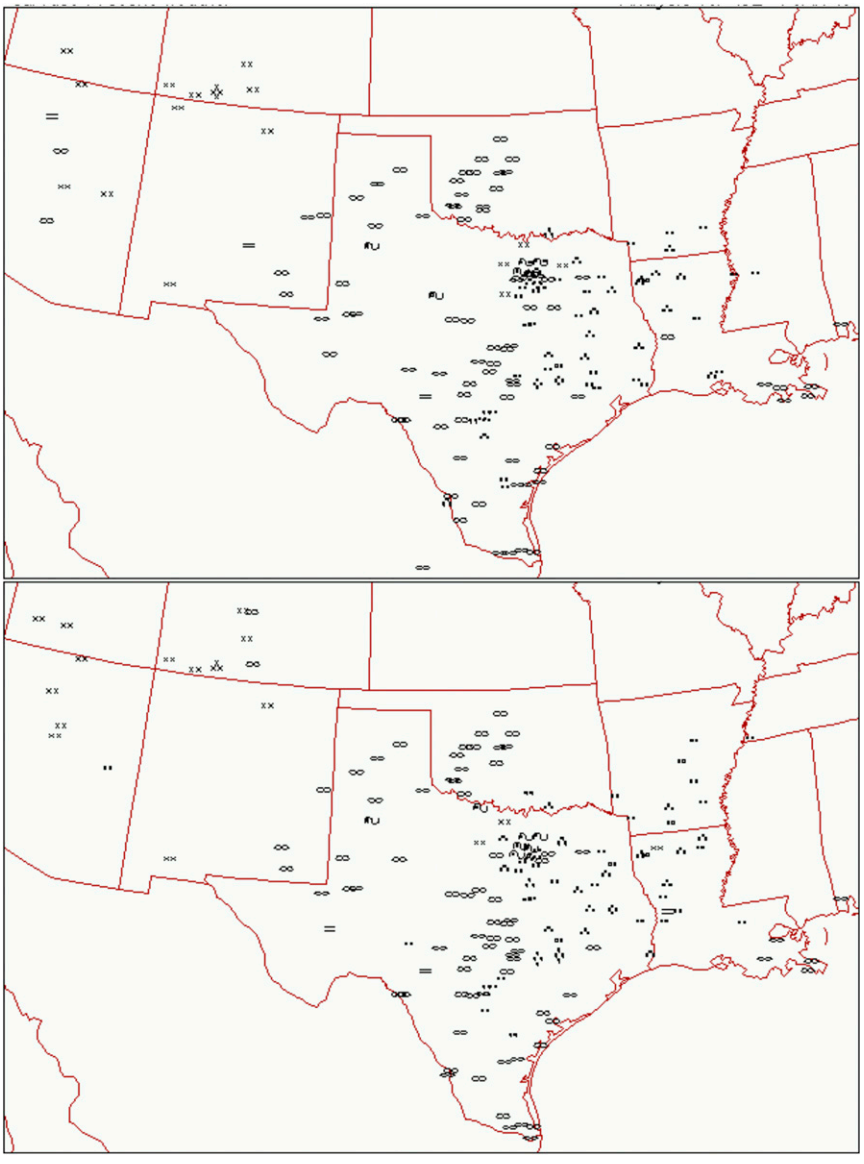

FIG. 4. Surface present weather observations including precipitation type valid at (top) 1500 and (bottom) 1600 UTC 1 Jan 2015 (courtesy of Plymouth State University; http://vortex.plymouth.edu/myo/sfc/pltmap-a.html). Weather symbols are described online (http://www.meteor.wisc.edu/~hopkins/aos100/sfc-anl.htm).

addition, the fall rate for graupel is greater than that for rain, IP only is diagnosed, not FZ and not rain. If the 2-m temperature is >3°C, IP is not diagnosed, thus not allowing IP to include the condition of convectively produced hail.

b. *Rationale for explicit precipitation-type diagnosis*

Although the model generally produces a dominant precipitation type, in the difficult cases of cold-season mixed precipitation, simply using the precipitation types directly from the model without any qualification as to the surface accumulation rate of that particular species leads to a confusing picture when displayed as a superposition of binary (0/1) fields. This is because at 2-m temperatures not far from 0°C, the physical solution within a multispecies microphysics scheme can give small amounts of more than one hydrometeor species falling to the surface in the model. Thus, it was necessary to introduce postprocessing logic into the classification scheme for appropriate thresholds of the multispecies fall rate.

Thresholds for SF and 2-m temperature in the precipitation-type diagnostic logic were subjectively

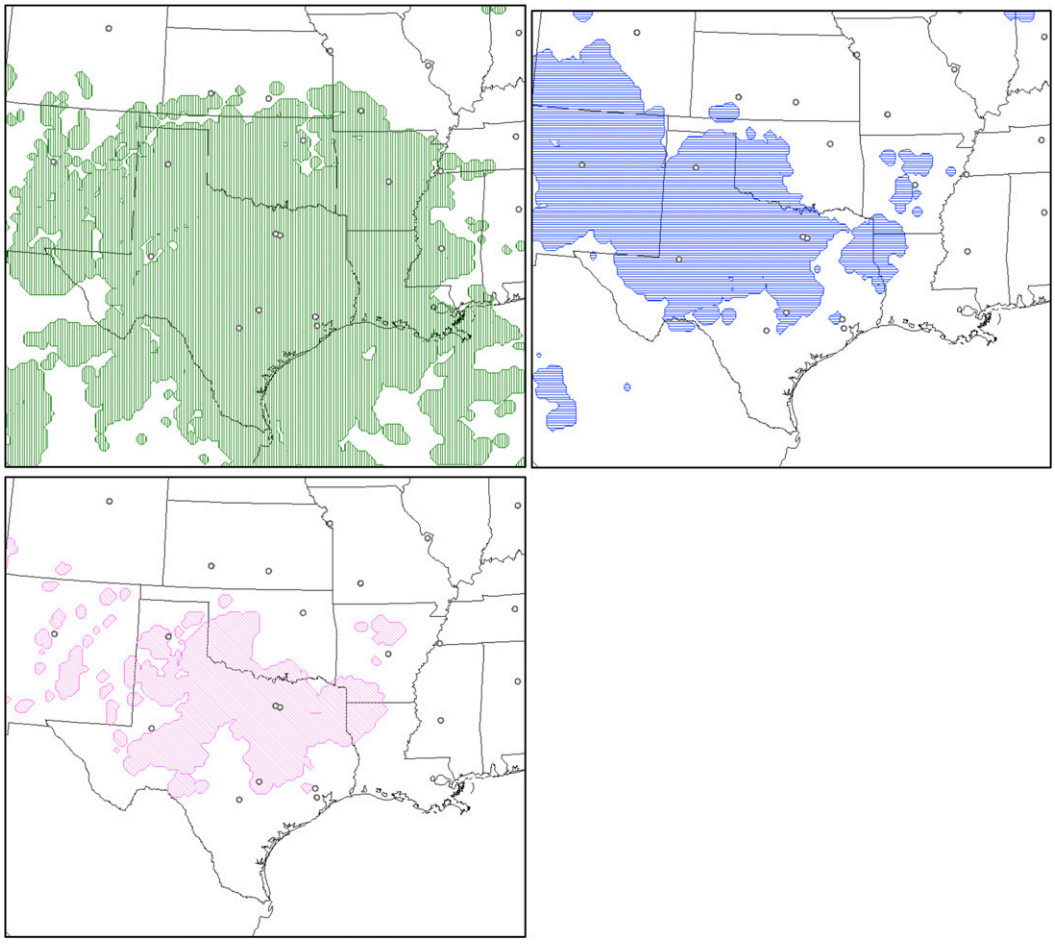

FIG. 5. As in Fig. 3, but for areas of nonzero 1-h precipitation in the form of (top left) rain, (top right) snow, and (bottom) graupel.

estimated (no effect on the actual forecast model solution) against observations of precipitation type from Automated Surface Observing System (ASOS) reports to avoid the problem of diagnosing too large (or too small) areal coverage of mixed precipitation (e.g., rain/snow or freezing rain/ice pellets/snow). It is also necessary to make use of the model forecast of the 2-m temperature to identify situations where rain is falling at temperatures < 0°C, and to limit the IP diagnosis to formation in cold-season storms and exclude convectively produced hail. Allowing snow precipitation-type identification with 2-m temperatures up to 1°C accounts for the wet-bulb effect, which is already identified in the Thompson et al. microphysics via energy exchange between snow and environmental air as the snow falls at its fall speed.

To increase the likelihood of successfully predicting freezing drizzle at the surface, the more recent Thompson et al. microphysics schemes (Thompson et al. 2008; Thompson and Eidhammer 2014) include a two-moment rain component in order to better describe the collision–coalescence process in clouds that are mainly composed of liquid particles but at temperatures < 0°C throughout the cloud depth.

We also note that the precipitation rates used currently for the model explicit precipitation-type diagnosis are 1) instantaneous and 2) have a minimum threshold ($0.0001\ \text{mm h}^{-1}$) much lighter than sensible by current measurement methods. The use of the instantaneous precipitation rates means that this diagnostic method could be expanded into higher-frequency products or into a future PDF precipitation-type field. The very small precipitation rate thresholds were designed to capture very light drizzle or light snow events, even at the expense of showing a bias versus ASOS-level sensitivity for precipitation types (not shown). Thériault et al. (2006) and Thériault and Stewart (2010) considered a precipitation-type fraction but did not

address how to approximate observer guidelines for yes/no precipitation-type identification.

4. Case study and 2013–15 validation

a. Case example

A brief example is shown to illustrate application of the explicit precipitation-type diagnosis in Figs. 2–4 for a winter storm forecast valid at 1600 UTC 1 January 2015. Figure 2 shows precipitation type diagnosed from an RAP (13 km) 1-h forecast with areas of snow, freezing rain, and ice pellets from New Mexico across northern Texas with rain over southern Texas. Smaller areas of mixed precipitation types are shown from northern Texas to the Arkansas–Louisiana border in the 1-h forecast with the explicit precipitation-type diagnosis, including *S*–FZ, FZ–IP, and *R*–IP mixtures. The total 1-h precipitation is added in Fig. 2b, indicating the superset of possible areas for precipitation-type assignment (gray) and areas of heavier precipitation (>0.1 in. h^{-1} in light green), usually for rain but some for FZ and IP. A breakdown of each precipitation-type forecast area is added in Fig. 3 to see the specific coverage areas of each precipitation type. The METAR observations of precipitation type valid at the forecast valid time are shown in Fig. 4. Freezing rain observations in Fig. 4 are generally within the FZ forecast area evident in Figs. 2 and 3. The rain–snow line in the observations (Fig. 4) is very close to that diagnosed for the 1-h RAP forecast. Some snow and FZ reports are shown in the Dallas–Fort Worth, Texas, area (Fig. 4), similar to the mixed *S*–FZ area forecast just west of those cities. A freezing rain report (Fig. 4) at 1500 UTC in central Texas (Abilene) was covered by the forecast FZ area in Figs. 2 and 3. Freezing rain and drizzle was diagnosed near but not covering the Lubbock FZ report in western Texas. The areal coverage in the forecast, especially for snow and freezing rain, is larger than shown in the observations, because of the very light precipitation threshold of 0.0001 mm h^{-1}, well below the measurable minimum of about 0.25 mm h^{-1}. Areas of 1-h precipitation (supersets of the areas of instantaneous precipitation) are also shown for rain, snow, and graupel in Fig. 5, the starting point for the algorithm. The value added of applying the explicit precipitation-type algorithm can be seen in comparing Fig. 5 with Fig. 3 (and in Fig. 2b). The precipitation-type algorithm identifies areas of FZ and limits the *R*, *S*, and IP assignment by the temperature, precipitation intensity, and other constraints shown in the logic flow in Fig. 1 and described in section 3.

For comparison with another precipitation-type diagnostic, Fig. 6 shows the results from the dominant precipitation type (Manikin 2005) combining Baldwin et al., Ramer, Bourgouin, and revised Baldwin et al. techniques using gridded data from the same RAP 1-h forecast shown in Figs. 2 and 3 for the explicit precipitation-type diagnostic described in this paper. The general coverage is slightly larger with the dominant precipitation type in Fig. 6 (any precipitation greater than zero qualifies). The dominant precipitation type (Fig. 6) also shows a significant area of ice pellets in western Texas not shown with the explicit precipitation-type diagnosis. A sounding for Lubbock (Fig. 7) from the same common RAP 1-h forecast grid used for both precipitation-type diagnoses indicates a saturated level above 0°C that could support IP, although the explicit precipitation type based on Thompson et al. microphysics indicated snow with occasional mixed FZ. Observations from 1400 to 1900 UTC showed only FZ and *S* observations in western Texas (only 1600 UTC; shown in Fig. 4). Generally, fewer details are shown in Fig. 6 (dominant) than Fig. 2 (explicit), including the freezing rain in western Texas and snow reports near the Dallas area. The dominant precipitation-type scheme also cannot show mixed precipitation, by definition, but this condition is diagnosed with the explicit precipitation-type scheme in Fig. 2 in some areas in northern Texas. This comparison is qualitative and suggests that the explicit precipitation-type diagnosis is credible.

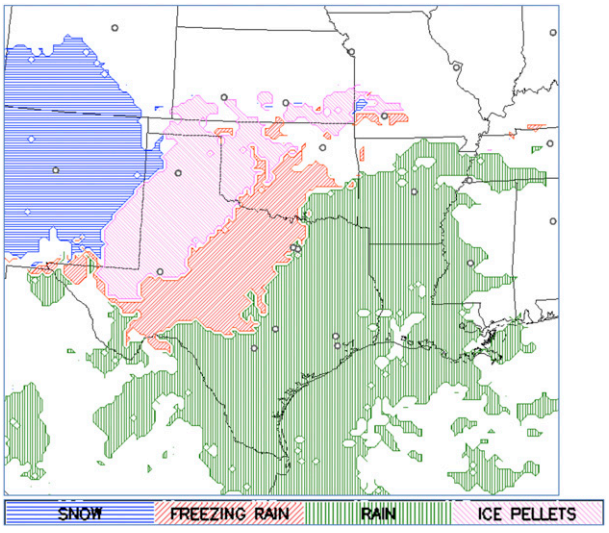

FIG. 6. As in Fig. 2, but for the dominant precipitation-type diagnostic (Manikin 2005) combining Baldwin et al., Ramer, Bourgouin, and revised Baldwin et al. diagnostics.

b. Validation of explicit 1-h precipitation-type forecasts from HRRR and RAP

Probability of detection for 1-h RAP (ESRL experimental) precipitation-type forecasts is presented in Fig. 8 over a 28-month period including two full winter

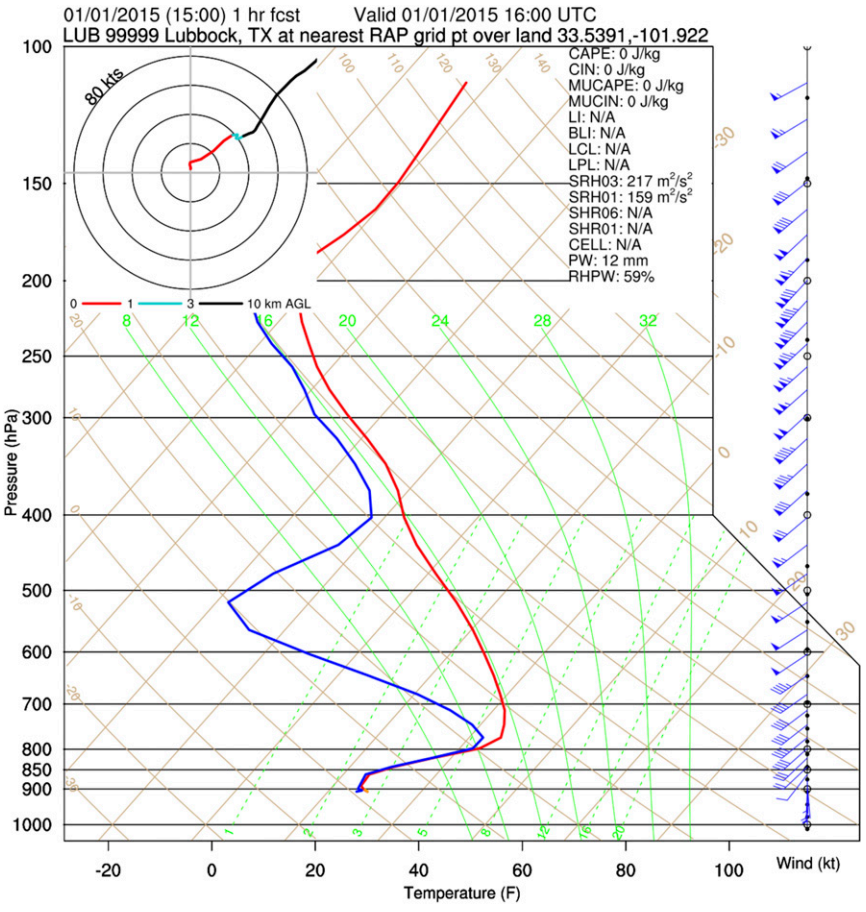

FIG. 7. Sounding skew T–log$P$ profile of temperature and moisture at Lubbock for the 1-h RAP forecast valid at 1600 UTC, the same RAP run shown in Figs. 2 and 5.

seasons using the nearest 13-km RAP grid point to the METAR observation location. The probability of detection for occurrence events (PODy) is ~0.9 in all of the 24 months over the conterminous United States for rain and about 0.8–0.9 for snow over the same period during winter months. The PODy for IP ranges from 0.3 to 0.55 (most common month—February) and slightly lower for FZ. The PODy for IP from this diagnostic is far higher than that shown in Elmore et al. (2015) who used RAP results not including the IP algorithm change in the ESRL version in January 2013. Both IP and FZ usually occur in geographically limited areas, so high PODy is difficult to achieve in real-data modeling. The deficiency in PODy for IP and FZ is likely due to errors in temperature, water vapor, and hydrometeor initialization. The number of IP and FZ events is rare: for instance, during February 2015, for METARs within the CONUS area including southern Canada, the total number of reports was about 60 000 for snow, 30 000 for rain, 2000 for freezing drizzle/rain, and 400 for ice pellets. As mentioned at the end of section 3, the precipitation-type diagnostic method uses a minimum threshold (0.0001 mm h^{-1}) that is much lighter than detectable by current measurement methods (minimum 0.25 mm h^{-1}), resulting in a high false alarm ratio (FAR) versus METAR observations (Fig. 9).[2] The overall FAR for measurable (0.25 mm) precipitation for RAP versus METARs is depicted in Fig. 10, showing an overall FAR of about 0.35–0.40, much lower than that shown in Fig. 9 with the far lower threshold for the precipitation-type algorithm designed to capture very light but significant freezing precipitation events.

5. Conclusions

The explicit precipitation-type diagnostic scheme described here is a relatively new approach applicable with

[2] It should be noted that the ASOS used at METAR sites currently does not have the ability to detect IP. This precipitation type is nominally only reported when an ASOS observation is augmented by a human observer, partially accounting for the paucity of IP reports.

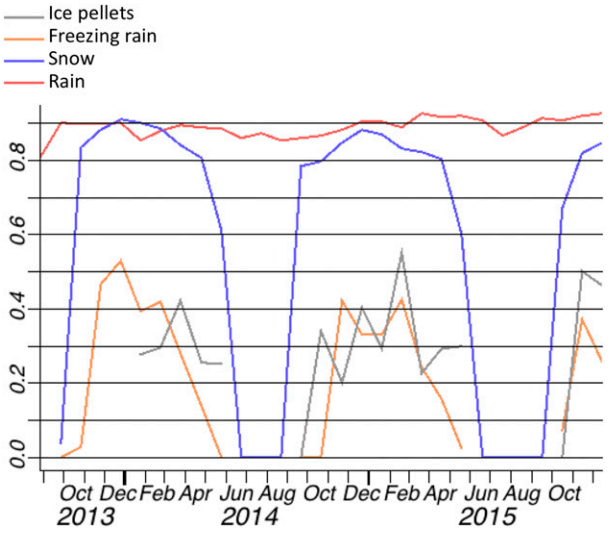

FIG. 8. Probability of detection for four different precipitation types [rain (red), snow (blue), freezing rain/drizzle (orange), and ice pellets (gray)] from 1-h forecasts from the ESRL experimental 13-km RAP as verified against METAR observations vs the nearest single 13-km grid points. Results are averaged over 30-day periods over the period from 15 Aug 2013 through 15 Dec 2015.

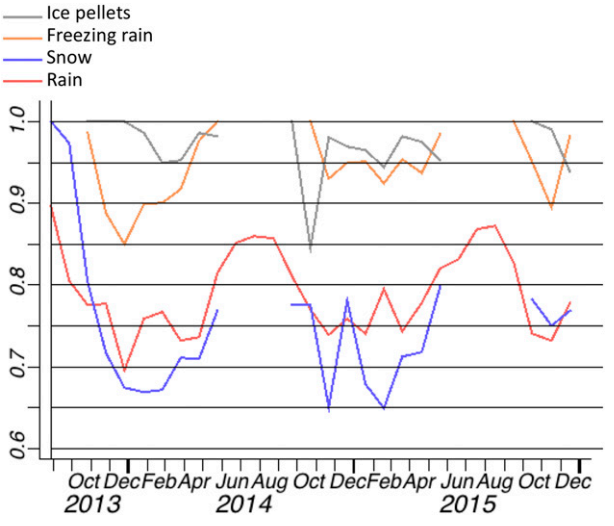

FIG. 9. As in Fig. 8, but for FAR. The explicit precipitation type is applied for 1-h precipitation as low as 0.0001 mm h^{-1} to capture very light freezing precipitation whereas METAR observation precision is limited to a min of 0.25 mm h^{-1}.

explicit model forecasts of rain, snow, and graupel precipitation at the surface. This scheme has been applied to NOAA operational models that use the Thompson et al. cloud and precipitation microphysics, specifically, the HRRR and RAP, and before 2012, with the RUC. This scheme was shown to provide effective results in a 2-yr evaluation and in a winter storm case study. This scheme has been used at NCEP in its hourly updated models (RUC, RAP, and HRRR) since 2005.[3]

This explicit diagnosis of precipitation type from the RAP and HRRR is directly linked with the multispecies cloud microphysics. Uncertainty in forecast thermodynamic structure is obviously a source of error in precipitation-type forecasts using this diagnostic method, as shown for other methods (Thériault et al. 2006; Reeves et al. 2014). Probabilistic precipitation-type forecasts are an obvious extension of this explicit precipitation-type algorithm, using time-lagged and explicit ensembles of RAP, HRRR, and/or other models with multispecies cloud microphysics schemes. Explicit precipitation-type forecasting accuracy is expected to further improve with assimilation of dual-polarization radar with diagnostic of hydrometeor type, a direction being taken in RAP and HRRR data assimilation development.

It should be noted that the algorithm discussed here is intended for wintertime application. The Thompson et al. microphysics scheme (both the 2008 and 2014 versions) does not have a separate hail category but, in situations conducive to deep convection, will sometimes produce graupel precipitation during the warm season when used within cloud-permitting forecast models such as the HRRR. Work to introduce a hail-size algorithm into the Thompson et al. microphysics for warm-season forecast applications will be discussed elsewhere.

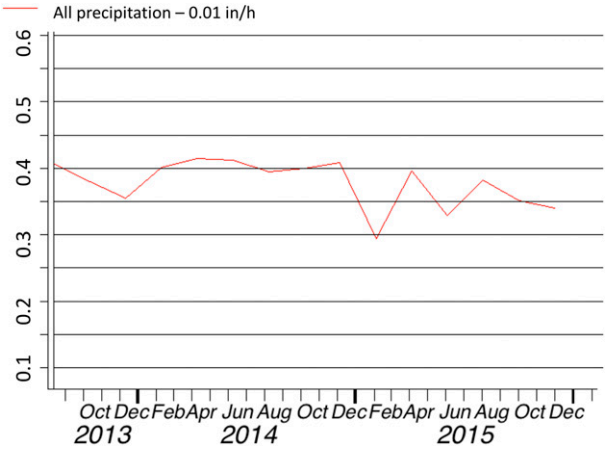

FIG. 10. As in Fig. 9, but for 1-h total precipitation of at least 0.01 in. h^{-1} (0.25 mm h^{-1}). Values are for 60-day averages.

[3] Occurrence of mixed snow/rain was excessively diagnosed with this scheme until a correction to a snow fraction error in January 2011. The scheme as described here, including the January 2011 correction also noted in Ikeda et al. (2013), was incorporated into the initial implementation of the RAP at NCEP on 1 May 2012.

Acknowledgments. We thank Joseph Koval at The Weather Company and Kyoko Ikeda and her NCAR colleagues for their help in identifying problems with the precipitation-type diagnosis that led to improvements in the scheme now documented in this article. We also thank Greg Thompson at the National Center for Atmospheric Research for ongoing collaboration, and colleagues at NOAA/ESRL, especially Curtis Alexander and Brian Jamison, for their help on evaluation of the precipitation-type algorithm described here. We thank Kim Elmore and his colleagues at NSSL for prompting identification of need for the IP criterion resetting. Ongoing changes in the precipitation-type diagnostic described in this paper are tracked online (http://ruc.noaa.gov/rr/RAP_var_diagnosis.html#ptype). Finally, we thank Trevor Alcott, David Dowell, and John Osborn (NOAA/ESRL) for very helpful reviews. The Federal Aviation Administration has partially supported some of this work.

REFERENCES

Baldwin, M., R. Treadon, and S. Contorno, 1994: Precipitation type prediction using a decision tree approach with NMC's Mesoscale Eta Model. Preprints, *10th Conf. on Numerical Weather Prediction*, Portland, OR, Amer. Meteor. Soc., 30–31.

Benjamin, S. G., G. A. Grell, J. M. Brown, and T. G. Smirnova, 2004a: Mesoscale weather prediction with the RUC hybrid isentropic-terrain-following coordinate model. *Mon. Wea. Rev.*, **132**, 473–494, doi:10.1175/1520-0493(2004)132<0473:MWPWTR>2.0.CO;2.

——, and Coauthors, 2004b: An hourly assimilation–forecast cycle: The RUC. *Mon. Wea. Rev.*, **132**, 495–518, doi:10.1175/1520-0493(2004)132<0495:AHACTR>2.0.CO;2.

——, and Coauthors, 2016: A North American hourly assimilation and model forecast cycle: The Rapid Refresh. *Mon. Wea. Rev.*, doi:10.1175/MWR-D-15-0242.1, in press.

Bocchieri, J. R., 1979: A new operational system for forecasting precipitation type. *Mon. Wea. Rev.*, **107**, 637–649, doi:10.1175/1520-0493(1979)107<0637:ANOSFF>2.0.CO;2.

——, 1980: The objective use of upper air soundings to specify precipitation type. *Mon. Wea. Rev.*, **108**, 596–603, doi:10.1175/1520-0493(1980)108<0596:TOUOUA>2.0.CO;2.

——, and G. J. Maglaras, 1983: An improved operational system for forecasting precipitation type. *Mon. Wea. Rev.*, **111**, 405–419, doi:10.1175/1520-0493(1983)111<0405:AIOSFF>2.0.CO;2.

Bourgouin, P., 2000: A method to determine precipitation types. *Wea. Forecasting*, **15**, 583–592, doi:10.1175/1520-0434(2000)015<0583:AMTDPT>2.0.CO;2.

DeGaetano, A. T., B. N. Belcher, and P. L. Spier, 2008: Short-term ice accretion forecasts for electric utilities using the Weather Research and Forecasting Model and a modified precipitation-type algorithm. *Wea. Forecasting*, **23**, 838–853, doi:10.1175/2008WAF2006106.1.

Elmore, K. L., H. M. Grams, D. Apps, and H. D. Reeves, 2015: Verifying forecast precipitation type with mPING. *Wea. Forecasting*, **30**, 656–667, doi:10.1175/WAF-D-14-00068.1.

Ikeda, K., M. Steiner, J. Pinto, and C. A. Alexander, 2013: Evaluation of cold-season precipitation forecasts generated by the hourly updating High-Resolution Rapid Refresh model. *Wea. Forecasting*, **28**, 921–939, doi:10.1175/WAF-D-12-00085.1.

Keeter, K. K., and J. W. Cline, 1991: The objective use of observed and forecast thickness values to predict precipitation type in North Carolina. *Wea. Forecasting*, **6**, 456–469, doi:10.1175/1520-0434(1991)006<0456:TOUOOA>2.0.CO;2.

Manikin, G. S., 2005: An overview of precipitation type forecasting using NAM and SREF data. Preprints, *21st Conf. on Weather Analysis and Forecasting/17th Conf. on Numerical Weather Prediction*, Washington, DC, Amer. Meteor. Soc., 8A.6. [Available online at https://ams.confex.com/ams/pdfpapers/94838.pdf.]

Office of Federal Coordinator for Meteorology, 2005: Federal Meteorological Handbook No. 1—Surface Weather Observations and Reports. [Available online at http://www.ofcm.gov/fmh-1/fmh1.htm.]

Ramer, J., 1993: An empirical technique for diagnosing precipitation type from model output. Preprints, *Fifth Int. Conf. on Aviation Weather Systems*, Vienna, VA, Amer. Meteor. Soc., 227–230.

Reeves, H. D., K. L. Elmore, A. Ryzhkov, T. Schuur, and J. Krause, 2014: Sources of uncertainty in precipitation-type forecasting. *Wea. Forecasting*, **29**, 936–953, doi:10.1175/WAF-D-14-00007.1.

Schuur, T. J., H.-S. Park, A. V. Ryzhkov, and H. D. Reeves, 2012: Classification of precipitation types during transitional winter weather using the RUC model and polarimetric radar retrievals. *J. Appl. Meteor. Climatol.*, **51**, 763–779, doi:10.1175/JAMC-D-11-091.1.

Smith, T. L., S. G. Benjamin, J. M. Brown, S. Weygandt, T. Smirnova, and B. Schwartz, 2008: Convection forecasts from the hourly updated, 3-km High Resolution Rapid Refresh (HRRR) Model. Preprints, *24th Conf. on Severe Local Storms*, Savannah, GA, Amer. Meteor. Soc., 11.1. [Available online at https://ams.confex.com/ams/pdfpapers/142055.pdf.]

Thériault, J. M., and R. E. Stewart, 2010: A parameterization of the microphysical processes forming many types of winter precipitation. *J. Atmos. Sci.*, **67**, 1492–1508, doi:10.1175/2009JAS3224.1.

——, ——, and W. Henson, 2006: On the dependence of winter precipitation types on temperature, precipitation rate, and associated features. *J. Appl. Meteor. Climatol.*, **49**, 1429–1442, doi:10.1175/2010JAMC2321.1.

Thompson, G., and T. Eidhammer, 2014: A study of aerosol impacts on clouds and precipitation development in a large winter cyclone. *J. Atmos. Sci.*, **71**, 3636–3658, doi:10.1175/JAS-D-13-0305.1.

——, R. M. Rasmussen, and K. Manning, 2004: Explicit forecasts of winter precipitation using an improved bulk microphysics scheme. Part I: Description and sensitivity analysis. *Mon. Wea. Rev.*, **132**, 519–542, doi:10.1175/1520-0493(2004)132<0519:EFOWPU>2.0.CO;2.

——, P. R. Field, R. M. Rasmussen, and W. D. Hall, 2008: Explicit forecasts of winter precipitation using an improved bulk microphysics scheme. Part II: Implementation of a new snow parameterization. *Mon. Wea. Rev.*, **136**, 5095–5115, doi:10.1175/2008MWR2387.1.

Vislocky, R. L., and G. S. Young, 1989: The use of perfect prog forecasts to improve model output statistics forecasts of precipitation probability. *Wea. Forecasting*, **4**, 202–209, doi:10.1175/1520-0434(1989)004<0202:TUOPPF>2.0.CO;2.

Wagner, A. J., 1957: Mean temperature from 1000 to 500 mb as a predictor of precipitation type. *Bull. Amer. Meteor. Soc.*, **10**, 584–590.

Wandishin, M. S., M. E. Baldwin, S. L. Mullen, and J. V. Cortinas Jr., 2005: Short-range ensemble forecasts of precipitation type. *Wea. Forecasting*, **20**, 609–626, doi:10.1175/WAF871.1.